

---

# Comparison of L-[1-<sup>11</sup>C]Methionine and L-Methyl-[<sup>11</sup>C]Methionine for Measuring In Vivo Protein Synthesis Rates with PET

Kiichi Ishiwata, Willem Vaalburg, Philip H. Elsinga, Anne M. J. Paans, and Martien G. Woldring

*Department of Nuclear Medicine, University Hospital, Groningen, The Netherlands*

To evaluate the feasibility of using either L-[1-<sup>11</sup>C]-methionine or L-[methyl-<sup>11</sup>C]methionine for measuring protein synthesis rates by positron emission tomography (PET) in normal and neoplastic tissues, distribution and metabolic studies with <sup>14</sup>C- and <sup>11</sup>C-labeled methionines were carried out in rats bearing Walker 256 carcinosarcoma. The tissue distributions of the two <sup>14</sup>C-labeled methionines were similar except for liver tissue. Similar distribution patterns were observed in vivo by PET using <sup>11</sup>C-labeled methionines. The highest <sup>14</sup>C incorporation rate into the protein-bound fraction was found in the liver followed by tumor, brain, and pancreas. The incorporation rates in liver and pancreas were different for the two methionines. By chloroform-methanol fractionation of these four tissues, in liver significantly different amounts of <sup>14</sup>C were observed in macromolecules. Also in brain tissue slight differences were found. By HPLC analyses of the protein-free fractions of plasma, tumor, and brain tissue at 60 min after injection, for both methionines several <sup>14</sup>C-labeled metabolites in different amounts, were detected. About half of the <sup>14</sup>C-labeled material in the protein-free fraction was found to be methionine. In these three tissues the amount of nonprotein metabolites and [<sup>14</sup>C]bicarbonate amount ranged from 10% to 17% and 12% to 15% for L-[1-<sup>14</sup>C]methionine and L-[methyl-<sup>14</sup>C]methionine, respectively. From these results it can be concluded that the minor metabolic pathways have to be investigated in order to quantitatively model the protein synthesis by PET.

J Nucl Med 29:1419-1427, 1988

---

**P**ositron emission tomography (PET) offers the opportunity for quantitative in vivo measurement of amino acid metabolism and protein synthesis rates (PSR) in tissues. For PSR measurements a combination of positron-emitting amino acids and appropriate mathematical models is necessary. A number of positron-emitting amino acids has been synthesized and used for animal and clinical studies. Since the first report of Comar et al. (1) on L-[methyl-<sup>11</sup>C]methionine most attention has been paid to this amino acid. Clinically, this amino acid has been applied to investigate brain disorders like Alzheimer's disease (2) and in the studies

of brain (3-8) and lung tumors (9). There is no doubt about the clinical usefulness of L-[methyl-<sup>11</sup>C]methionine for tumor visualization, but for quantitative measurements of PSR by PET, several problems are unresolved. Although the main metabolic pathway of L-[methyl-<sup>11</sup>C]methionine is protein incorporation, the influence of minor metabolic pathways on measuring PSR is under discussion (10,11). For instance, in brain L-methionine is a precursor of S-adenosyl-L-methionine (12) which plays an important role in biochemical transmethylation processes (13,14).

By using carboxylic labeled methionine, potential problems with the transmethylation pathway can be circumvented (15,16). In this case the label is expected to be incorporated partly into proteins and partly by decarboxylation, <sup>11</sup>CO<sub>2</sub> is diluted in the CO<sub>2</sub>-bicarbonate pool and removed rapidly from the tissue. In the process of the transmethylation, the <sup>11</sup>C-label of S-adenosyl-L-[1-<sup>11</sup>C]methionine is converted to S-adenosyl-L-[1-<sup>11</sup>C]homocysteine (17), which is a precursor of

---

Received July 1, 1987; revision accepted Mar. 8, 1988.  
For reprints contact: W. Vaalburg, MD, Dept. of Nuclear Medicine, University Hospital, Oostersingel 59, 9713 EZ Groningen, The Netherlands.  
Dr. K. Ishiwata is on leave of absence from the Division of Radioisotope Research, Cyclotron and Radioisotope Center, Tohoku University, Sendai, 980, Japan.

protein and methionine synthesis. In our previous studies with carbon-14 ( $^{14}\text{C}$ )carboxylic labeled tyrosine, the rapid removal of the  $^{14}\text{CO}_2$ - $^{14}\text{C}$ bicarbonate from tissue was confirmed (Ishiwata K, Vaalburg W, Elsinga PH, et al: unpublished data). Recently, we developed a method for the preparation of optically pure L-[ $^{11}\text{C}$ ]methionine (18). In this communication, we report on the tissue distribution in tumor-bearing rats of methionine labeled with  $^{14}\text{C}$  in the methyl and carboxyl position respectively and on PET studies with the carbon-11 ( $^{11}\text{C}$ )analogs.

## MATERIALS AND METHODS

D,L-[ $^{11}\text{C}$ ]Methionine was synthesized by the isocyanide method using  $^{11}\text{CO}_2$  as described previously (16). The D- and L-enantiomers were separated on  $\mu$ Bondapak C18 (Radial-Pak C18, Waters) with a sodium acetate buffer containing L-proline and copper acetate as eluent (18). L-[Methyl- $^{11}\text{C}$ ]methionine was synthesized by the reaction of  $^{11}\text{CH}_3\text{I}$  and L-homocysteine thiolactone according to the method of Comar et al. (1). L-[ $^{14}\text{C}$ ]Methionine (The Radiochemical Centre, Amersham, Buckinghamshire, UK) with a specific activity of 59 mCi/mmol, L-[methyl- $^{14}\text{C}$ ]methionine (Amersham) with a specific activity of 55 mCi/mmol and NCS (Amersham), a tissue solubilizer, were purchased commercially.

### Tumor-Bearing Rats

Male Wistar rats, weighing 200–250 g, with a transplantable Walker 256 carcinosarcoma were prepared by intramuscular injection of  $10^6$  tumor cells in the left hind leg, as described previously (19). Within 14 days after transplantation tumors were palpable.

### Measurement of Tissue Distribution and Expired $^{14}\text{CO}_2$

The tissue level of  $^{14}\text{C}$  radioactivity and the expired  $^{14}\text{CO}_2$  were measured. Each individual rat was kept in an acrylic cylinder and injected intravenously with  $^{14}\text{C}$ -labeled methionine. Expired  $^{14}\text{CO}_2$  was absorbed in NCS solution. The rats were killed at 5, 10, 15, 30, and 60 min after injection. Blood was removed using a syringe pre-coated with heparin and subsequently the blood was centrifuged for 5 min at 2,000 g to collect plasma. Brain, heart, lung, liver, pancreas, spleen, kidney, muscle, and tumor were dissected and washed with physiological saline. From the tumor necrotic regions were removed carefully. The tissue samples were dissolved in NCS solution and the  $^{14}\text{C}$  radioactivity was measured. The tissue uptake was expressed as the differential absorption ratio (DAR), (counts/g tissue)  $\times$  (g body weight/total injected counts). Expired  $^{14}\text{CO}_2$  absorbed in the NCS solution was also measured.

### Metabolic Studies

In order to investigate the metabolism of the  $^{14}\text{C}$ -labeled methionines, the presence of [ $^{14}\text{C}$ ]bicarbonate, the incorporation of  $^{14}\text{C}$  into the protein-bound fraction, and the proportion of intact [ $^{14}\text{C}$ ]methionine in the protein-free fraction of several tissues were measured. For the measurement of [ $^{14}\text{C}$ ]bicarbonate, plasma and tissue homogenates of tumor and brain tissue were treated with trichloroacetic acid. The generated  $^{14}\text{CO}_2$  was absorbed in NCS solution. Also plasma and

tissue homogenates of tumor, brain, pancreas, and liver were treated with trichloroacetic acid and the protein-bound and protein-free fractions were separated.

Measurement of [ $^{14}\text{C}$ ]methionine in the protein-free fraction was carried out by HPLC and liquid scintillation counting. The protein-free trichloroacetic acid solution was applied on a Aminex A-7 (BioRad Laboratories, Richmond, CA) column (0.48 cm ID  $\times$  15 cm). The column was used at 70°C and eluted with 0.2 N sodium citrate at a flow rate of 1.0 ml/min. The pH of the applied citrate buffer was changed stepwise: 30 ml at pH 3.00, 30 ml at pH 3.25 and 20 ml at pH 5.28. Fractions of 1.5 ml were collected and the  $^{14}\text{C}$  was measured in each fraction.

To compare the characteristics of the metabolites, the protein-bound and protein-free fractions of tumor, brain, pancreas and liver tissue were treated with chloroform-methanol (20). Tissue samples of 30 to 100 mg were treated with 1 ml 5% trichloroacetic acid. A separation between acid-precipitable (APF) and acid-soluble fractions (ASF) was achieved. The APF was mixed thoroughly with 1 ml  $\text{CHCl}_3$ — $\text{CH}_3\text{OH}$  (1:1). This mixture was centrifuged at 3,500 g for 5 min, to separate the precipitate (fraction A) and the  $\text{CHCl}_3$ — $\text{CH}_3\text{OH}$  extract. The extraction procedure was repeated two more times. The combined organic extract was washed once with 3 ml  $\text{CHCl}_3$ — $\text{H}_2\text{O}$  (1:1) and centrifuged as described above. Solid material appeared on the border of the organic and aqueous phase. This solid material and the aqueous layer were combined (fraction B) and separated from the organic layer (fraction C).

The ASF was extracted with three times the volume of  $\text{CHCl}_3$ — $\text{CH}_3\text{OH}$  (1:1). The mixture was centrifuged to separate the aqueous phase and the organic phase. This extraction was repeated two more times. The combined organic solutions were extracted with an equal volume of  $\text{CHCl}_3$ — $\text{H}_2\text{O}$  (1:1). The mixture was centrifuged to separate the organic solution (fraction D) and the aqueous solution. The aqueous solutions were combined (fraction E). The  $^{14}\text{C}$  content in the five fractions A to E was measured.

### Positron Emission Tomography

Tumor-bearing rats, anesthetized with pentobarbital (6 mg/100 g body weight), were injected intravenously with no-carrier-added L-[ $^{11}\text{C}$ ]methionine or L-[methyl- $^{11}\text{C}$ ]methionine (50–100  $\mu\text{Ci}$ , 2–4 MBq), and the distribution of the  $^{11}\text{C}$  was measured tomographically as a function of time using a stationary double-headed positron camera (22). After injection with L-[ $^{11}\text{C}$ ]methionine the distribution was followed for 1 hr in order to obtain insight in the kinetic behavior of the amino acid. After 2 hr of rest, the L-[methyl- $^{11}\text{C}$ ]methionine was injected and again a dynamic study lasting 1 hr was performed. A time difference of 9 half-lives, a factor of 500 was considered to be sufficient to exclude any influence of the former study on the latter. After correction of the images for the physical half-life of  $^{11}\text{C}$  the biologic behavior of both methionines are directly displayed by the images. In Fig. 3 both distributions in the rat are shown at 30 min after injection.

## RESULTS

The results of the tissue distribution studies with L-[ $^{14}\text{C}$ ]methionine in rats bearing Walker 256 carcinosarcoma are shown in Table 1. During the first 10 min

**TABLE 1**  
Tissue Distribution of L-[1-<sup>14</sup>C]Methionine in Rats Bearing Walker 256 Carcinosarcoma at Different Times After i.v. Injection

	Uptake (DAR) Tumor-to-tissue ratio				
	5 min (n = 5) <sup>*</sup>	10 min (n = 5)	15 min (n = 5)	30 min (n = 5)	60 min (n = 5)
Blood	0.73 ± 0.13 3.17	0.49 ± 0.04 7.49	0.40 ± 0.05 6.63	0.45 ± 0.06 6.51	0.67 ± 0.10 4.55
Plasma	0.86 ± 0.13 2.69	0.54 ± 0.05 6.81	0.44 ± 0.04 6.01	0.55 ± 0.12 5.48	0.89 ± 0.20 3.44
Brain	0.65 ± 0.11 3.62	0.57 ± 0.08 6.51	0.57 ± 0.04 4.58	0.67 ± 0.08 4.40	0.54 ± 0.04 5.61
Heart	1.50 ± 0.24 1.54	1.24 ± 0.23 2.97	1.19 ± 0.10 2.22	1.15 ± 0.09 2.56	1.06 ± 0.07 2.88
Lung	1.62 ± 0.41 1.42	1.36 ± 0.19 2.72	1.20 ± 0.09 2.20	1.35 ± 0.12 2.18	1.15 ± 0.16 2.64
Liver	3.59 ± 0.72 0.64	3.32 ± 0.98 1.11	3.51 ± 0.31 0.75	3.24 ± 0.73 0.91	2.91 ± 0.20 1.05
Pancreas	9.54 ± 2.10 0.24	8.59 ± 1.31 0.43	8.47 ± 1.92 0.31	8.71 ± 1.09 0.34	8.87 ± 1.98 0.35
Spleen	3.11 ± 0.46 0.74	2.72 ± 0.37 1.35	2.80 ± 0.47 0.94	3.16 ± 0.53 0.93	2.67 ± 0.22 1.14
Kidney	3.60 ± 0.69 0.64	3.47 ± 0.44 1.06	2.95 ± 0.29 0.89	3.05 ± 0.34 0.94	2.76 ± 0.33 1.10
Muscle	0.52 ± 0.10 4.39	0.65 ± 0.05 5.70	0.65 ± 0.15 4.02	0.60 ± 0.10 4.87	0.63 ± 0.11 4.88
Tumor	2.30 ± 0.83 1.00	3.68 ± 0.78 1.00	2.63 ± 0.97 1.00	2.94 ± 0.15 1.00	3.05 ± 1.09 1.00

<sup>\*</sup> n = Number of rats.  
Errors are s.d.

after injection of L-[1-<sup>14</sup>C]methionine, blood clearance was very rapid. After 15 min the <sup>14</sup>C level in blood increased gradually. In plasma the <sup>14</sup>C level was slightly higher than in whole blood; the clearance profile was similar. The highest uptake was found in the pancreas, in which the <sup>14</sup>C level was nearly constant with time. Also the liver showed a high uptake. After 15 min the <sup>14</sup>C level in this organ decreased slightly. In brain the <sup>14</sup>C level was low and nearly equal to the level in muscle. In Walker 256 carcinosarcoma a high accumulation of <sup>14</sup>C was found. In Table 1, the tumor-to-organ ratios are also presented. Tumor-to-blood, tumor-to-brain, and tumor-to-muscle ratios were high. Tumor-to-lung and tumor-to-heart ratios were medium. Tumor-to-other organs ratios were low.

In Table 2, the results of the tissue distribution studies with L-[methyl-<sup>14</sup>C]-methionine are presented. Compared with the results seen with carboxylic-labeled methionine, several differences were observed. The <sup>14</sup>C level in blood and plasma showed the same profile as for L-[1-<sup>14</sup>C]methionine but the uptake of the methyl labeled methionine was lower. Again, the pancreas showed the highest uptake; the <sup>14</sup>C level was lower. In liver the <sup>14</sup>C level was nearly constant.

To estimate the protein incorporation of <sup>14</sup>C-labeled methionine in the different tissues, the percentage of

the total tissue activity bound into protein of tumor, brain, pancreas and liver was measured (Table 3). The percentage of protein-bound <sup>14</sup>C in these tissues increased with time for both <sup>14</sup>C-labeled methionines. For both methionines the highest incorporation rate of radioactivity into protein was found for liver followed by tumor tissue. In tumor and brain tissue for both labeled methionines the PSR was similar. For both methionines a significant difference in protein incorporation was observed for liver and pancreas. In the liver at 5 min after injection of L-[methyl-<sup>14</sup>C]methionine 71% of the <sup>14</sup>C was already measured in the protein-bound fraction. The corresponding figure for carboxylic-labeled methionine was only 47%. In case of pancreas after injection of L-[1-<sup>14</sup>C]methionine the percentage of protein-bound <sup>14</sup>C increased with time. At 30 min and at 60 min after injection of methyl-labeled methionine, the percentages of the protein-bound <sup>14</sup>C were nearly equal and significantly smaller than those for L-[1-<sup>14</sup>C]methionine. The presence of protein-bound <sup>14</sup>C in the plasma is also shown in Table 3. For both labeled methionines the percentage of protein-bound <sup>14</sup>C increased rapidly after 15 min. The radioactivity incorporation in plasma proteins was higher for L-[1-<sup>14</sup>C]methionine than for L-[methyl-<sup>14</sup>C]methionine.

To investigate the washout of <sup>14</sup>CO<sub>2</sub>-[<sup>14</sup>C]bicarbonate

**TABLE 2**  
Tissue Distribution of L-[Methyl-<sup>14</sup>C]Methionine in Rats Bearing Walker 256 Carcinoma at Different Times After i.v. Injection

	Uptake (DAR) Tumor-to-tissue ratio		
	5 min (n = 3) <sup>*</sup>	30 min (n = 3)	60 min (n = 5)
	Blood	0.65 ± 0.11 1.58	0.41 ± 0.01 5.06
Plasma	0.73 ± 0.14 1.37	0.39 ± 0.07 5.35	0.68 ± 0.07 3.95
Brain	0.53 ± 0.05 1.89	0.54 ± 0.02 3.79	0.57 ± 0.05 4.77
Heart	1.07 ± 0.13 0.94	1.01 ± 0.21 2.03	1.06 ± 0.16 2.55
Lung	1.28 ± 0.15 0.78	1.05 ± 0.05 1.96	1.45 ± 0.30 1.86
Liver	3.40 ± 0.20 0.29	4.81 ± 0.33 <sup>†</sup> 0.43	4.96 ± 0.36 <sup>‡</sup> 0.54
Pancreas	7.37 ± 3.08 0.14	7.92 ± 1.24 0.26	7.35 ± 2.18 0.37
Spleen	2.19 ± 0.33 0.46	3.00 ± 0.33 0.69	2.80 ± 0.48 0.96
Kidney	2.45 ± 0.30 0.41	2.90 ± 0.07 0.71	3.39 ± 0.37 0.80
Muscle	0.46 ± 0.07 2.19	0.51 ± 0.05 4.02	0.63 ± 0.22 4.27
Tumor	1.00 ± 0.54 1.00	2.06 ± 0.59 1.00	2.70 ± 0.37 1.00

<sup>\*</sup> n = Number of rats

Errors are s.d.

A Student's t-test (compared to Table 1), <sup>†</sup> p < 0.01, <sup>‡</sup> p < 0.001

formed from decarboxylation and other minor metabolic pathways of labeled methionine, expired <sup>14</sup>CO<sub>2</sub> and the [<sup>14</sup>C]bicarbonate concentration in tissues were measured (Table 4). After injection of L-[<sup>14</sup>C]methi-

onine, the amount of expired <sup>14</sup>CO<sub>2</sub> increased linearly with time and 6% of total injected <sup>14</sup>C was measured at 60 min. In the case of L-[methyl-<sup>14</sup>C]methionine the amount was very low. The percentage of [<sup>14</sup>C]bicarbonate in plasma after injection of L-[<sup>14</sup>C]methionine increased during the first 15 min, followed by a decrease. In tumor and brain samples the [<sup>14</sup>CO]bicarbonate pool was found to be negligible (below 0.1% of the total <sup>14</sup>C level in these tissues). For L-[Methyl-<sup>14</sup>C]methionine, the level of [<sup>14</sup>C]bicarbonate in plasma was low.

To measure <sup>14</sup>C-labeled methionine in plasma and tissue samples, the protein-free fractions were applied to an Aminex A-7 column. High performance liquid chromatography (HPLC) chromatograms of plasma, tumor, and brain samples at 60 min after injection of L-[<sup>14</sup>C]methionine and L-[methyl-<sup>14</sup>C]-methionine respectively are shown in Fig. 1 and 2. In all chromatograms radioactive peaks with the same retention times are indicated with the same number. Peak 6 was identified as methionine by comparison with authentic L-[<sup>14</sup>C]- and L-[methyl-<sup>14</sup>C]-methionine. The retention time of peak 10 corresponded to that of S-adenosyl-L-methionine as measured by uv. The other peaks were not identified. The results are summarized in Table 5. In case of L-[<sup>14</sup>C]methionine, although HPLC profiles of three samples are similar, the relative percentages of metabolites were different. In plasma and tumor samples about half of the protein-free <sup>14</sup>C was found to be [<sup>14</sup>C]methionine. Peaks 1 and 5 were the predominant metabolites. In brain tissue 61% of the <sup>14</sup>C was identified as [<sup>14</sup>C]methionine. Peak 7 was found to be the predominant metabolite. On the other hand, the metabolic fate of L-[methyl-<sup>14</sup>C]methionine was more complicated. In plasma and brain, 57% and 64%, respectively, of the protein-free <sup>14</sup>C was observed in the [<sup>14</sup>C]methionine peak. The corresponding figure in tumor

**TABLE 3**  
Percentage of Total Tissue Radioactivity Incorporated into Proteins in Rat Tissues After Injection of L-[<sup>14</sup>C]Methionine or L-[Methyl-<sup>14</sup>C]-Methionine<sup>\*</sup>

		5 min	10 min	15 min	30 min	60 min
Tumor	1- <sup>14</sup> C-Met	47.5 ± 8.6	66.5 ± 6.8	67.4 ± 4.3	74.6 ± 3.1	79.7 ± 4.3
	Me- <sup>14</sup> C-Met	42.0 ± 4.6 <sup>†</sup>			72.4 ± 2.7 <sup>†</sup>	76.8 ± 3.9
Brain	1- <sup>14</sup> C-Met	23.3 ± 1.3	36.8 ± 1.7	47.1 ± 2.8	58.0 ± 0.6	68.5 ± 1.8
	Me- <sup>14</sup> C-Met	26.01 ± 2.2 <sup>†</sup>			58.0 ± 3.5 <sup>†</sup>	66.8 ± 3.7
Pancreas	1- <sup>14</sup> C-Met	23.5 ± 3.3	37.1 ± 7.7	44.9 ± 9.8	63.6 ± 8.3 <sup>‡</sup>	75.9 ± 3.4 <sup>‡</sup>
	Me- <sup>14</sup> C-Met	25.6 ± 5.6 <sup>†</sup>			44.9 ± 1.7 <sup>†</sup>	46.1 ± 3.3
Liver	1- <sup>14</sup> C-Met	46.9 ± 5.3 <sup>‡</sup>	64.7 ± 3.3	76.7 ± 2.9	83.7 ± 0.8 <sup>‡</sup>	87.0 ± 1.3 <sup>‡</sup>
	Me- <sup>14</sup> C-Met	71.3 ± 2.7 <sup>†</sup>			89.6 ± 1.2 <sup>†</sup>	86.6 ± 0.9
Plasma	1- <sup>14</sup> C-Met	1.7 ± 0.4	3.1 ± 0.6	8.5 ± 2.1	50.1 ± 10.7	80.2 ± 1.0
	Me- <sup>14</sup> C-Met	4.4 ± 0.7 <sup>†</sup>			36.2 ± 8.3 <sup>†</sup>	70.3 ± 4.2

<sup>\*</sup> 1-<sup>14</sup>C-Met and Me-<sup>14</sup>C-Met represent L-[<sup>14</sup>C]methionine and L-[methyl-<sup>14</sup>C]methionine, respectively.

Data indicate an average of five or three samples (†).

Errors are s.d.

A Student's t-test was carried out for the data of the two methionines, <sup>‡</sup> p < 0.001

**TABLE 4**  
Expired  $^{14}\text{CO}_2$  and Levels of [ $^{14}\text{C}$ ]Bicarbonate in Plasma of Rats After Injection of L-[1- $^{14}\text{C}$ ]Methionine or L-[Methyl- $^{14}\text{C}$ ]Methionine\*

	$^{14}\text{CO}_2$ , % of total injected $^{14}\text{C}$				
	5 min	10 min	15 min	30 min	60 min
1- $^{14}\text{C}$ -Met	0.24 ± 0.09	0.71 ± 0.19	1.09 ± 0.33	2.46 ± 0.44	5.87 ± 2.19
Me- $^{14}\text{C}$ -Met	0.04 ± 0.01†			0.22 ± 0.05†	0.95 ± 0.70

	[ $^{14}\text{C}$ ]Bicarbonate, % of total $^{14}\text{C}$ in plasma				
	5 min	10 min	15 min	30 min	60 min
1- $^{14}\text{C}$ -Met	4.1 ± 0.4	4.8 ± 1.1	11.3 ± 3.4	8.2 ± 2.6	3.1 ± 0.5
Me- $^{14}\text{C}$ -Met	1.5 ± 0.7†			2.8 ± 0.3†	0.6 ± 0.2

\* 1- $^{14}\text{C}$ -Met and Me- $^{14}\text{C}$ -Met represent L-[1- $^{14}\text{C}$ ]methionine and L-[methyl- $^{14}\text{C}$ ]methionine, respectively.

$^{14}\text{CO}_2$  expired and absorbed in NCS solution during indicated periods after the injection of methionine.

Data indicate an average of five or three rats (†).

Errors are s.d.

samples was only 37%. In tumor tissue peak 4 was a predominant metabolite; in plasma and brain samples peak 4 was very small. In these samples peak 5 was the predominant metabolite.

In Table 6 the results of chloroform-methanol fractionation of tissues are presented. Several characteristics were observed. In tumor tissue the percentage of the five fractions were similar for both labeled methionines. Significant amounts of the protein-bound  $^{14}\text{C}$  and the protein-free  $^{14}\text{C}$  were extracted with chloroform-methanol. In brain tissue the percentages in the fraction B and the fraction C in experiments with L-[1- $^{14}\text{C}$ ]methionine, were smaller than in experiments with L-[methyl- $^{14}\text{C}$ ]methionine. Compared to other tissues, in pancreas the percentages in the fraction C and the fraction D were very small. The distribution pattern of the radioactivity over the five fractions depends on the position of the label in the amino acid. In liver the percentage in fraction A was very small, especially in the studies with L-[methyl- $^{14}\text{C}$ ]methionine and about one-half of the  $^{14}\text{C}$  was detected in the fraction C. For pancreas tissue the percentage of fraction C was low.

In vivo distribution studies with L-[1- $^{11}\text{C}$ ]methionine and with L-[methyl- $^{11}\text{C}$ ]methionine were carried out by PET. In Figure 3 the distribution of both labeled amino acids in the same rat is presented. High accumulation of  $^{11}\text{C}$  was observed in the abdominal region. Especially in the liver with L-[methyl- $^{11}\text{C}$ ]methionine the  $^{11}\text{C}$  accumulation was higher than with L-[1- $^{11}\text{C}$ ]methionine. Accumulation of  $^{11}\text{C}$  in the brain and in the tumor transplanted in the left hind leg, was observed clearly with both labeled methionines. The uptake level for brain and tumor tissue were similar for both labeled methionines. The tumor muscle ratio, as determined from left and right hind leg, was 2 or more for both methionines.

## DISCUSSION

Quantitative in vivo measurement of PSR or amino acid metabolism in normal tissue like brain and pancreas as well as in tissues with disorders, e.g., tumors, is an objective for PET studies. From clinical point of view, up to now most attention has been paid to L-[methyl- $^{11}\text{C}$ ]methionine. Methionine is an interesting amino acid; it is an essential amino acid with a small free pool in tissue. Moreover, the preparation method is not too complex and it has a high radiochemical yield. In brain or tumor studies, after injection of this  $^{11}\text{C}$ -amino acid the accumulation of  $^{11}\text{C}$  radioactivity reflects the metabolism of methionine, probably protein synthesis. For quantitative in vivo measurement of the PSR in brain tissue, Bustany et al. proposed a kinetic model without taking into account minor metabolic pathways, e.g., decarboxylation and transmethylation (2). However, there are several reports describing minor metabolic pathways (2,10,11) such as the conversion of methyl-labeled methionine to S-adenosyl-L-methionine. It is expected that this pathway can be circumvented by using  $^{11}\text{C}$ -carboxylic labeled methionine. In this report, we compared the tissue distribution and metabolism of carboxylic and methyl labeled methionines in tumor-bearing rats.

In the tissue distribution studies with these two differently labeled methionines, a significant difference of radioactivity uptake in the liver was observed (Tables 1 and 2). After injection of methyl-labeled methionine, the  $^{14}\text{C}$  level increased with time. For carboxylic-labeled methionine the  $^{14}\text{C}$  level decreased. Also the protein incorporation rate of  $^{14}\text{C}$  in liver tissue differed; for L-[methyl- $^{14}\text{C}$ ]methionine a higher rate was observed than for L-[1- $^{14}\text{C}$ ]methionine (Table 3). In plasma on the contrary, the protein-bound fraction was higher for

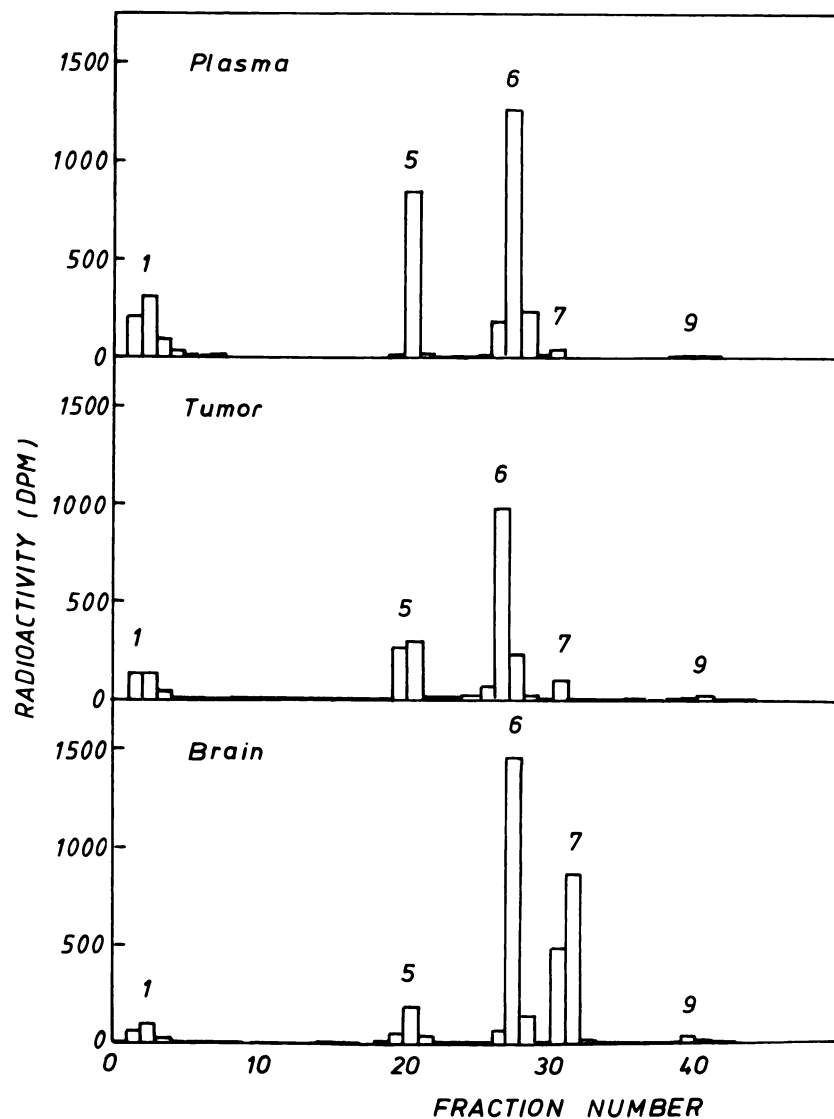


**FIGURE 1**  
HPLC analyses of protein-free  $^{14}\text{C}$ -metabolites in plasma, tumor and brain at 60 min after injection of L-[1- $^{14}\text{C}$ ]methionine.

carboxylic-labeled methionine than for methyl-labeled methionine. These results indicate that in case of L-[methyl- $^{14}\text{C}$ ]methionine a part of the protein-bound  $^{14}\text{C}$  in liver tissue was retained and not excreted in plasma. By PET studies similar liver accumulation patterns of  $^{11}\text{C}$  were observed using two  $^{11}\text{C}$ -labeled methionines (Fig. 3). It was interesting to follow the different fates of the two methionines as is presented by the chloroform-methanol fractionation (Table 6). In case of L-[methyl- $^{14}\text{C}$ ]methionine about a half of  $^{14}\text{C}$  was extracted with chloroform-methanol. This suggests that this  $^{14}\text{C}$  was incorporated into lipophilic macromolecules or lipids in membranes. The chloroform-methanol fractionation could discriminate the characteristics of the protein-bound  $^{14}\text{C}$  in tissues.

In the tumors, the protein incorporation rates and relative distributions of  $^{14}\text{C}$  were similar for the two methionines. In the case of brain tissue the rates were similar but were lower than in tumor tissue. In brain

tissue using chloroform-methanol fractionation, different distribution patterns were observed. The results show that the position of the label in the molecule determines the macromolecules labeled.

For the pancreas, the distributions measured by the chloroform-methanol fractionation method were similar for the two methionines. In case of L-[methyl- $^{14}\text{C}$ ]methionine the protein incorporation rate decreased after 30 min and at 60 min the amount of  $^{14}\text{C}$  in the protein-bound fraction was lower than for L-[1- $^{14}\text{C}$ ]methionine. This suggests that the specific activity of the  $^{14}\text{C}$ -labeled amino acid in the protein-free fraction decreased after 30 min. This assumption was confirmed by HPLC analyses (Table 5).

In accordance with Jones et al. (11), several nonprotein metabolites of L-[methyl- $^{14}\text{C}$ ]methionine were observed. The percentages of metabolites in plasma, tumor, and brain samples were different. In these tissues, the percentages of  $^{14}\text{C}$ -labeled methionine in the pro-

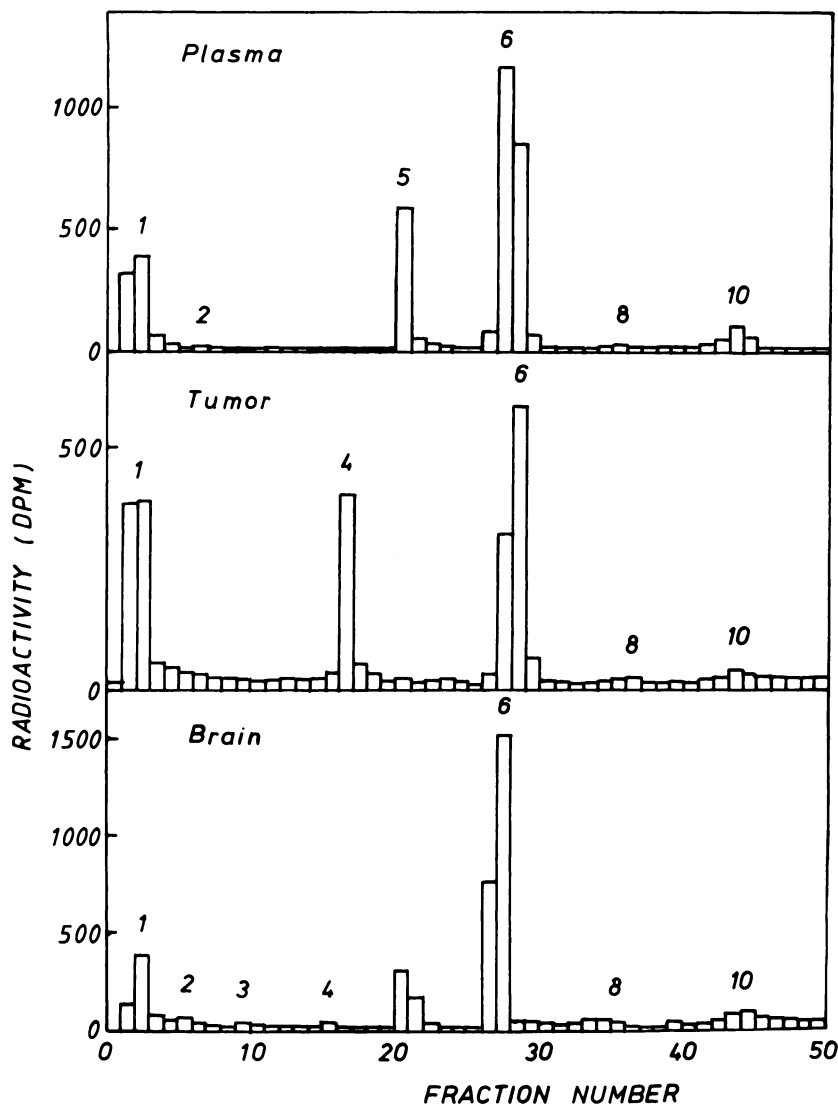


**FIGURE 2**  
HPLC analyses of protein-free  $^{14}\text{C}$ -metabolites in plasma, tumor and brain at 60 min after injection of L-[methyl- $^{14}\text{C}$ ]methionine.

**TABLE 5**  
HPLC Analysis of  $^{14}\text{C}$ -Labeled Metabolites in the Protein-Free Fraction of Rat Tissues at 60 min After Injection of L-[ $^{14}\text{C}$ ]Methionine or L-[Methyl- $^{14}\text{C}$ ]methionine

	% of the protein-free $^{14}\text{C}$					
	Peak 1	Peak 5	L-[ $^{14}\text{C}$ ]methionine Peak 6		Peak 7	Peak 9
Plasma	22.4 ± 2.3	27.9 ± 1.9	48.2 ± 4.4		1.1 ± 0.4	0.4 ± 0.3
Tumor	14.5 ± 3.6	30.6 ± 3.5	51.1 ± 4.0		2.7 ± 1.9	1.1 ± 0.6
Brain	5.3 ± 0.3	8.5 ± 1.8	61.2 ± 19.1		24.6 ± 17.3	0.5 ± 0.4
	L-[methyl- $^{14}\text{C}$ ]methionine					
	Peaks 1-3	Peak 4	Peak 5	Peak 6	Peak 8	Peak 10
Plasma	19.6 ± 0.8	0.2 ± 0.1	19.3 ± 2.1	57.2 ± 2.5	0.4 ± 0.1	3.4 ± 2.0
Tumor	40.6 ± 4.4	18.2 ± 2.6	0.6 ± 0.5	36.9 ± 6.5	0.7 ± 0.4	3.3 ± 3.5
Brain	16.0 ± 1.4	0.2 ± 0.1	10.3 ± 1.6	64.0 ± 8.7	1.6 ± 1.1	3.5 ± 3.1

Data indicate an average of three samples.  
Errors are s.d.

**TABLE 6**  
Chloroform-Methanol Fractionation of the  $^{14}\text{C}$  in Rat Tissues at 60 min After Injection of L-[1- $^{14}\text{C}$ ]Methionine or L-[Methyl- $^{14}\text{C}$ ]Methionine

		Protein-bound fraction			Protein-free fraction	
		Fraction A (%)	Fraction B (%)	Fraction C (%)	Fraction D (%)	Fraction E (%)
Tumor	1- $^{14}\text{C}$ -Met	37.0 ± 8.4	28.7 ± 8.1	12.3 ± 5.2	6.0 ± 0.4	16.0 ± 3.6
	Me- $^{14}\text{C}$ -Met	33.9 ± 6.3	30.5 ± 4.3	9.5 ± 4.8	6.0 ± 1.9	20.0 ± 1.9
Brain	1- $^{14}\text{C}$ -Met	25.5 ± 5.5 <sup>§</sup>	34.2 ± 4.3	7.6 ± 1.4 <sup>‡</sup>	8.1 ± 1.8	24.6 ± 1.4
	Me- $^{14}\text{C}$ -Met	13.9 ± 1.2	38.5 ± 2.3	11.5 ± 0.9	9.4 ± 2.2	26.8 ± 1.8
Pancreas	1- $^{14}\text{C}$ -Met	26.9 ± 2.2 <sup>‡</sup>	41.2 ± 10.1	1.1 ± 0.2	1.9 ± 0.4 <sup>§</sup>	28.8 ± 7.4 <sup>§</sup>
	Me- $^{14}\text{C}$ -Met	17.6 ± 3.1	33.2 ± 3.2	1.8 ± 0.6	0.9 ± 0.3	45.8 ± 3.6
Liver	1- $^{14}\text{C}$ -Met	12.7 ± 3.1 <sup>‡</sup>	70.3 ± 1.6 <sup>†</sup>	2.7 ± 0.5 <sup>†</sup>	1.4 ± 0.2	12.9 ± 1.0
	Me- $^{14}\text{C}$ -Met	4.1 ± 0.2	32.0 ± 1.6	48.9 ± 1.9	1.1 ± 0.2	13.9 ± 1.0

<sup>†</sup> 1- $^{14}\text{C}$ -Met and Me- $^{14}\text{C}$ -Met represent L-[1- $^{14}\text{C}$ ]methionine and L-[methyl- $^{14}\text{C}$ ]methionine, respectively.

Data indicate an average of three samples.

Errors are s.d.

A Student's t-test was carried out for the data of the two methionines, †  $p < 0.01$ , ‡  $p < 0.01$ , §  $p < 0.02$ .

tein-free fraction at 60 min after injection were below 64%. For L-[methyl- $^{14}\text{C}$ ]methionine, especially in tumor tissue, this figure was only 37%. From these results it can be concluded that the influence of the minor metabolic pathways have to be taken into account in designing a kinetic model for the quantitative measurement of PSR. We only identified  $^{14}\text{C}$ -labeled S-adenosyl-L-methionine in the HPLC chromatogram. We found a much lower percentage of this compound than Jones et al. In tissue, the  $^{14}\text{C}$ -methyl group of this compound is probably incorporated into the acid-precipitable fraction as shown in liver and kidney (20) as well as in tumor tissue (21). This type of  $^{14}\text{C}$  accumulation in the acid-precipitable fraction may reflect the incorporation into macromolecules via the transmethylation pathway. Although carboxyl-labeled methionine is a good prospect for the kinetic analysis of PSR (15,16), the metabolism is complicated (Table 5). The metabolism in tumor and brain tissue is different as shown by the different percentages of peaks 5 and 7. In tumor the percentage for L-[1- $^{14}\text{C}$ ]methionine is higher compared to L-[methyl- $^{14}\text{C}$ ]methionine. The corre-

sponding figures in plasma and brain tissues are similar to the figures of L-[methyl- $^{14}\text{C}$ ]methionine.

The results in Tables 3, 4, and 5 were summarized in Table 7. In our metabolic studies with L-[1- $^{14}\text{C}$ ]tyrosine, the percentages of total nonprotein metabolites in plasma, tumor, and brain at 60 min after injection were only 3.3%, 1.9%, and 3.7%, respectively, (unpublished data). Compared with the L-[1- $^{14}\text{C}$ ]tyrosine the influence of the minor metabolic pathways, when using L-[methyl- $^{14}\text{C}$ ]methionine, on the kinetic analysis of PSR is more prominent. It is possible that, with the combined potential of the two labeled methionines, insight can be obtained in the transmethylation process, especially in the liver.

In conclusion, the metabolic fate of L-[1- $^{14}\text{C}$ ]methionine or L-[methyl- $^{14}\text{C}$ ]methionine in the first 60 min after injection is different, especially in the liver. The presence of several metabolites in the protein-free fractions for both differently labeled methionines have to be accounted for in the kinetic model for the in vivo quantitative measurement of protein synthesis rates by PET.

**FIGURE 3**  
Positron emission tomography of a rat bearing Walker 256 carcinosarcoma after injection of L-[1- $^{11}\text{C}$ ]methionine and after 2 hr L-[methyl- $^{11}\text{C}$ ]methionine. The planar image was obtained by the positron camera (22). The head of the rat is on the left side of the image.

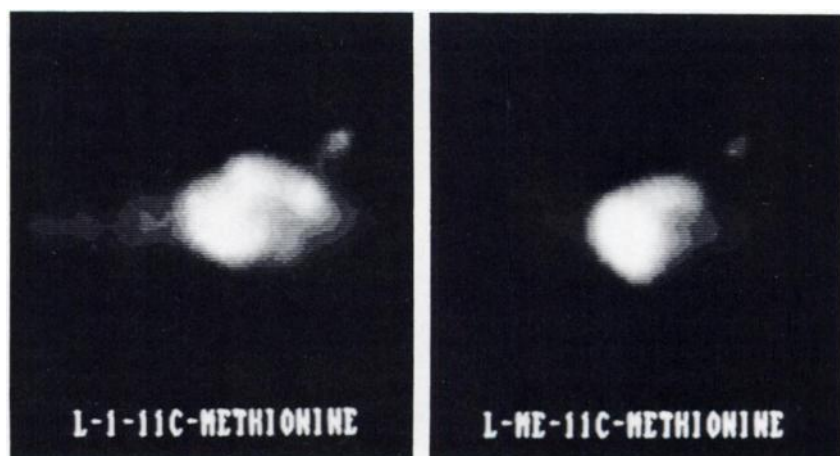


**TABLE 7**  
Relative Radioactivity in Plasma, Tumor, and Brain Tissues of Rats at 60 min After Injection of L-[1-<sup>14</sup>C]Methionine or L-[Methyl-<sup>14</sup>C]Methionine\*

		Protein-bound fraction (%)	Methionine (%)	Nonprotein metabolites (%)	Bicarbonate (%)
Plasma	1- <sup>14</sup> C-Met	80.2	8.0	8.7	3.1
	Me- <sup>14</sup> C-Met	70.3	16.6	12.5	0.6
Tumor	1- <sup>14</sup> C-Met	79.7	10.4	9.9	
	Me- <sup>14</sup> C-Met	76.8	8.6	14.6	
Brain	1- <sup>14</sup> C-Met	68.5	14.2	17.3	
	Me- <sup>14</sup> C-Met	66.8	21.2	12.0	

\* 1-<sup>14</sup>C-Met and Me-<sup>14</sup>C-Met represent L-[1-<sup>14</sup>C]methionine and L-[methyl-<sup>14</sup>C]methionine, respectively.

## ACKNOWLEDGMENTS

This research was supported by the Dutch Cancer Foundation "Koninging Wilhelmina Fonds". The authors acknowledge the cooperation of staff of the Kernfysisch Versneller Instituut (Prof. Dr. R.H. Siemssen) and the considerable help of the cyclotron operators.

## REFERENCES

- Comar D, Cartron JC, Maziere M, Marazano C. Labelling and metabolism of methionine-methyl-<sup>11</sup>C. *Eur J Nucl Med* 1976; 1:11-14.
- Bustany P, Henry JF, Soussaline F, Comar D. Brain protein synthesis in normal and demented patients—a study by positron emission tomography with <sup>11</sup>C-L-methionine. In: Magistretti PL, ed. *Functional radio-nuclide imaging of the brain*. New York: Raven Press, 1983: 319-326.
- Bergstrom M, Collins VP, Ehrin E, et al. Discrepancies in brain tumor extent as shown by computed tomography and positron emission tomography using [<sup>68</sup>Ga] EDTA, [<sup>11</sup>C]glucose, and [<sup>11</sup>C]-methionine. *J Comput Assist Tomogr* 1983; 7:1062-1066.
- Lilja A, Bergstrom K, Hartvig P, et al. Dynamic study of supratentorial gliomas with L-[methyl-<sup>11</sup>C]methionine and positron emission tomography (PET). *Am J Neurol Rad* 1985; 6:505-514.
- Meyer GJ, Schober O, Hundeshagen H. Uptake of <sup>11</sup>C-L- and D-methionine in brain tumors. *Eur J Nucl Med* 1985; 10:373-376.
- Schober O, Meyer GJ, Stolke D, Hundeshagen H. Brain tumor imaging using C-11-labeled L-methionine and D-methionine. *J Nucl Med* 1985; 26:98-99.
- Ericson K, Lilja A, Bergstrom M, et al. Positron emission tomography with <sup>11</sup>C-methyl-L-methionine, <sup>11</sup>C-D-glucose and <sup>68</sup>Ga-EDTA in supratentorial tumors. *J Comput Assist Tomogr* 1985; 9:683-689.
- Bustany P, Chatel M, Derlon JM, et al. Brain tumor protein synthesis and histological grades: a study by positron emission tomography (PET) with C11-L-methionine. *J Neuro Oncol* 1986; 3:397-404.
- Kubota K, Matsuzawa T, Ito M, et al. Lung tumor imaging by positron emission tomography using C-11 L-methionine. *J Nucl Med* 1985; 26:37-42.
- Lundqvist H, Stalnacke CG, Langstrom B, Jones B. Labeled metabolites in plasma after intravenous administration of [<sup>11</sup>CH<sub>3</sub>]-L-methionine. In: Greitz T, et al. eds. *The metabolism of the human brain studied with positron emission tomography*. New York: Raven Press, 1985: 233-240.
- Jones RM, Cramer S, Sargent T, Budinger TF. Brain protein synthesis rates measured in vivo using methionine and leucine [Abstract]. *J Nucl Med* 1985; 26: P 168.
- Baldessarini RJ, Kopin IJ. S-adenosyl-methionine in brain and other tissues. *J Neurochem* 1986; 13:769-777.
- Andreoli VM, Agnoli A, Fazio C, eds. *Transmethylation and the central nervous system*. Berlin, Heidelberg, New York: Springer-Verlag, 1978.
- Usdin E, Borchardt RT, Creveling CR eds. *Transmethylation*. New York, Amsterdam, Oxford: Elsevier/North-Holland, 1979.
- Phelps ME, Barrio JR, Huang SC, et al. Criteria for the tracer kinetic measurement of cerebral protein synthesis in humans with positron emission tomography. *Ann Neurol* 1984; 15:S192-S202.
- Bolster JM, Vaalburg W, Elsinga PH, et al. Synthesis of DL-[1-<sup>11</sup>C]methionine. *Appl Radiat Isot* 1986; 37:1069-1070.
- Lombardini JB, Talalay P. Formation, functions and regulatory importance of S-adenosyl-L-methionine. *Adv Enzyme Reg* 1971; 9:349-384.
- Bolster JM, Vaalburg W, Elsinga PH, et al. The preparation of <sup>11</sup>C-carboxylic labelled L-methionine for measuring protein synthesis. *J Label Comp* 1986; 23:1081-1082.
- Bolster JM, Vaalburg W, Paans AMJ, et al. Carbon-11 labelled tyrosine to study tumor metabolism by positron emission tomography (PET). *Eur J Nucl Med* 1986; 12:321-324.
- Ishiwata K, Ido T, Sato H, et al. Simplified enzymatic synthesis and biodistribution of <sup>11</sup>C-S-adenosyl-L-methionine. *Eur J Nucl Med* 1986; 11:449-452.
- Ishiwata K, Ido T, Abe Y, et al. Tumor uptake studies of S-adenosyl-L-[methyl-<sup>11</sup>C]methionine and L-[methyl-<sup>11</sup>C]methionine. *Nucl Med Biol*: in press.
- Paans AMJ, de Graaf EJ, Welleweerd J, et al. Performance parameters of a longitudinal tomographic positron imaging system. *Nucl Instrum Meth* 1982; 192:491-500.